Electronic Supplementary Material (ESI) for Physical Chemistry Chemical Physics.

Supporting Information

Probing heterogeneity of NIR induced secondary fluorescence from DNA-stabilized silver nanoclusters at the single molecule level.

Stefan Krause,* Miguel R. Carro-Temboury, Cecilia Cerretani, Tom Vosch.*

Nano-Science Center / Department of Chemistry, University of Copenhagen, Universitetsparken 5, 2100 Copenhagen, Denmark.

Materials and Methods.

DNA-AgNC synthesis. DNA-AgNCs were synthesized and HPLC purified as described previously by Cerretani et al.[1] The stock solution of DNA-AgNCs in 10 mM NH_4OAc was mixed with a solution of PVA (Aldrich) in MQ water to create the ensemble solution. For the single molecule measurements, the ensemble solution was further diluted with PVA in MQ water until it reached an adequate DNA-AgNC concentration for single molecule measurements ($\sim 10^{-9}$-10^{-10} M). Both PVA/DNA-AgNC solutions were spin cast onto an oven annealed glass coverslip (Menzel 630-1843).

Single molecule confocal fluorescence measurements. Single molecule measurements were performed with a home build confocal microscope.[2] We used the output of a pulsed white light laser (SuperK EXTREME EXB-6) which produces a continuous emission spectrum from 420 to 2400 nm. The spectrum was firstly filtered by a 950 nm short pass filter (Semrock) and a 488 nm long pass filter (Semrock Razor Edge). The residual spectrum was then separated into a short (primary) and long (secondary) wavelength part by a tunable long pass filter (Semrock Versachrome, TLP01-628) which was tilted to transmit light below 570 nm. This short wavelength part was further filtered by a 561 nm bandpass (Semrock MaxLine Laser Line) and a 633 nm short pass (Semrock) and adjusted to a primary excitation intensity of 3.7 kW/cm^2. The long wavelength part serving as secondary excitation beam was reduced to the wavelength region between 765 and 850 nm with a bandpass filter (Chroma ET810/90M) and send through a delay line resulting in a constant time delay of Δt = 27.67 ns with respect to the primary excitation pulse. The secondary excitation intensity was set to 85 kW/cm^2. Both beams were coaligned by transmission/reflection through a second tunable long pass filter (Semrock Versachrome, TLP01-628) and then reflected by a 30:70 beam splitter (XF122 Omega Optical) into an oil immersion objective (Olympus, UPlanSApo 100× NA = 1.4). The fluorescence signal was collected with the same objective. The primary and secondary excitation light was blocked by a 561 nm long pass filter (Semrock Edge Basic) and a 700 nm short pass filter (Chroma, ET700SP-2P8). The fluorescence signal was then detected by an avalanche photodiode (Perkin-Elmer CD3226) connected to a single photon counting module (Becker & Hickl SPC-830). Recording of spectra was achieved by inserting a 50:50 beam splitter and sending half of the fluorescence signal to a liquid nitrogen cooled spectrograph (Princeton Instruments SPEC-10:100B/LN_eXcelon CCD camera, SP 2356 spectrometer, 300 grooves/mm). This was done for 67 molecules of the 239 measured molecules. We like to point out that selection of molecules from the images was deliberately not random, but that there was a bias on the molecules with higher SF/PF ratio since we especially wanted to collect data on these DNA-AgNCs. This was done to get an idea of the range of possible single molecule behaviours and should not be used to calculate accurate population statistics. Data was analyzed with self-written Matlab algorithms.

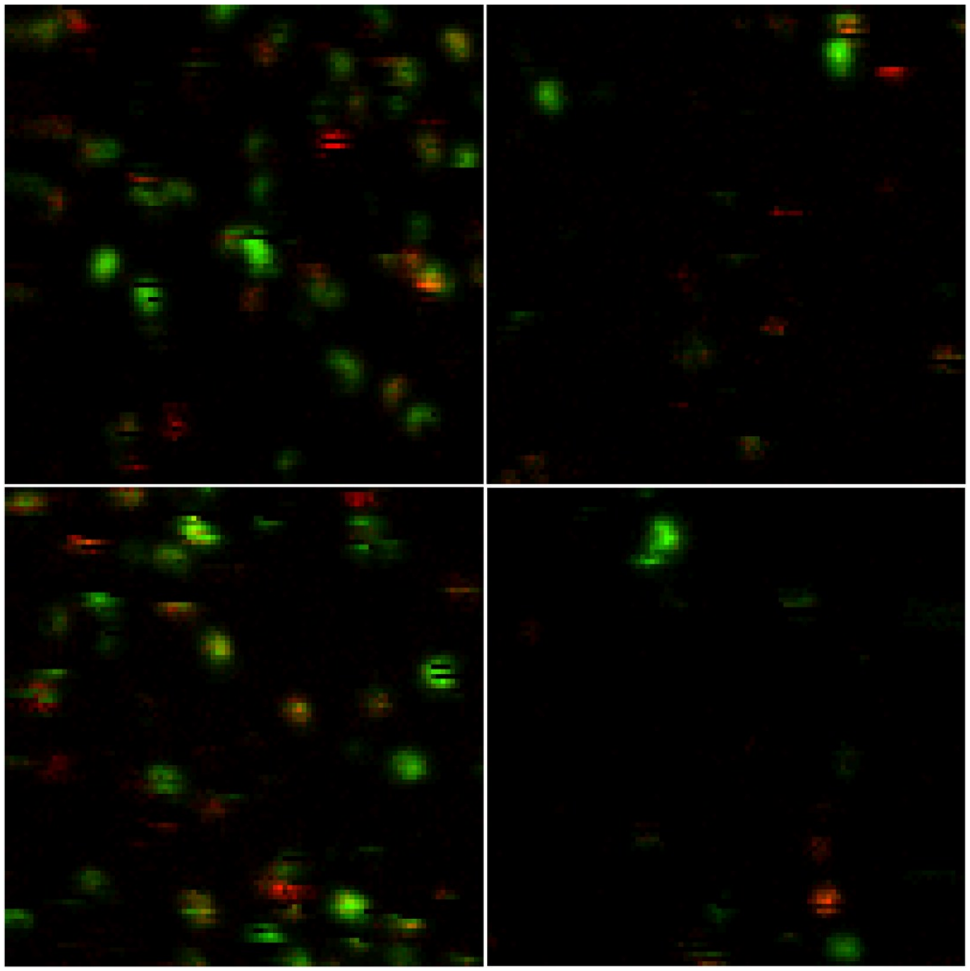

Figure S1: PArTI images of single DNA-AgNCs embedded in PVA (10 x 10 μm^2). As can be seen from Figure 1B and Figure 2A, the PF signal (green time channel) is usually much higher than the SF signal (red time channel). In the PArTI images shown here and in Figure 2B in the manuscript, the green and red time channels were normalized respectively to the highest PF and SF intensity value in each image, in order to increase the SF/PF contrast in the image. The actual SF/PF ratio images can be found in Figure S2.

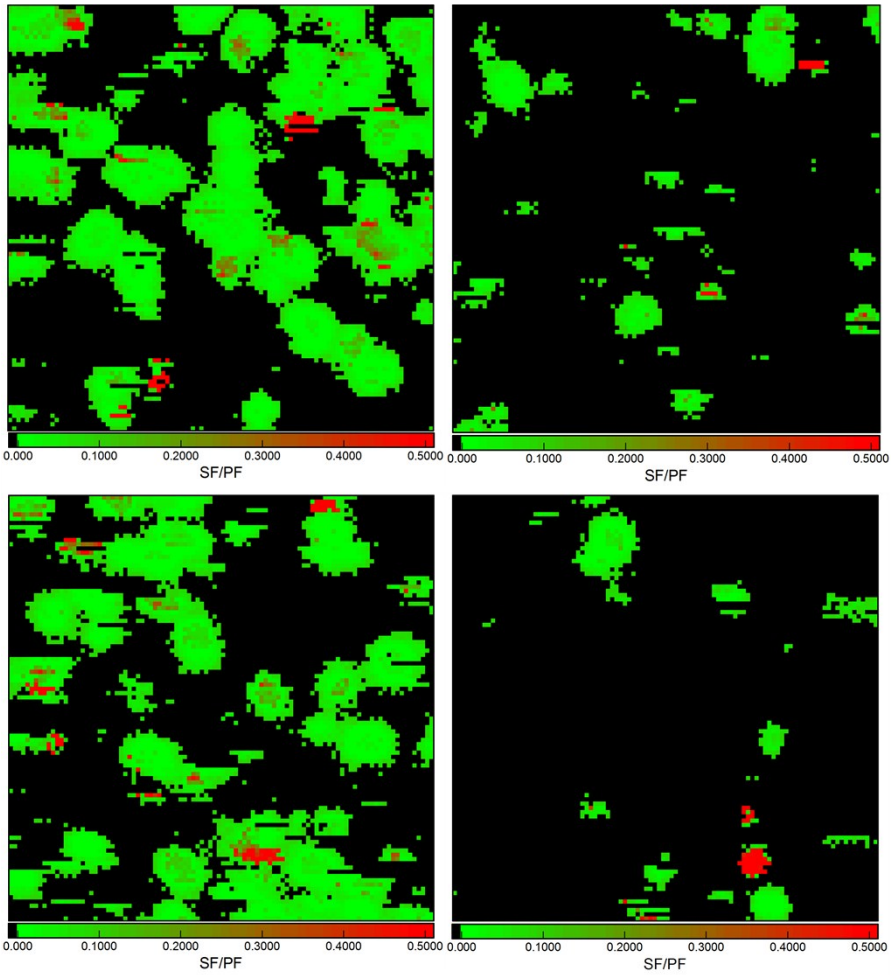

Figure S2: SF/PF ratio images of the single DNA-AgNCs shown in Figure S1 (10 x 10 μm^2). The images were constructed by dividing the pixel counts for SF by the pixel counts of the PF channel. A threshold of 10 counts was applied to both channels resulting in black regions where one or both channels have fewer counts. Note that the color scale has been adjusted to the range SF/PF = 0 - 0.5.

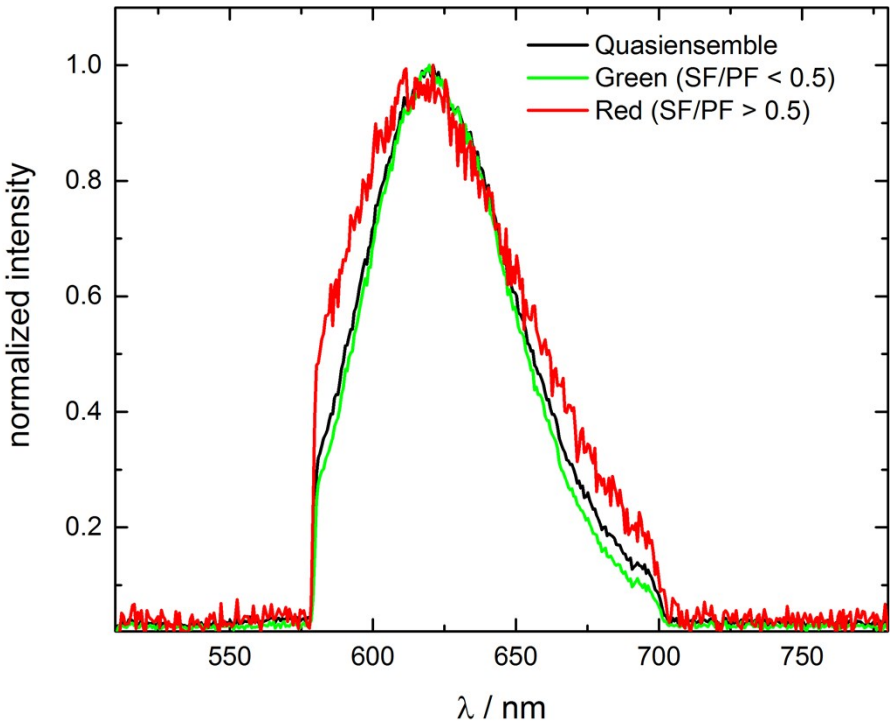

Figure S3: Sum spectra of all DNA-AgNCs (black, average of 67 molecules), sum spectra DNA-AgNCs with an SF/PF ratio below 0.5 (green, average of 51 molecules) and sum spectra DNA-AgNCs with an SF/PF ratio above 0.5 (red, average of 16 molecules). Short and long wavelength edges are a result of long pass (560 nm) and short pass (700 nm) filter cut off, respectively.

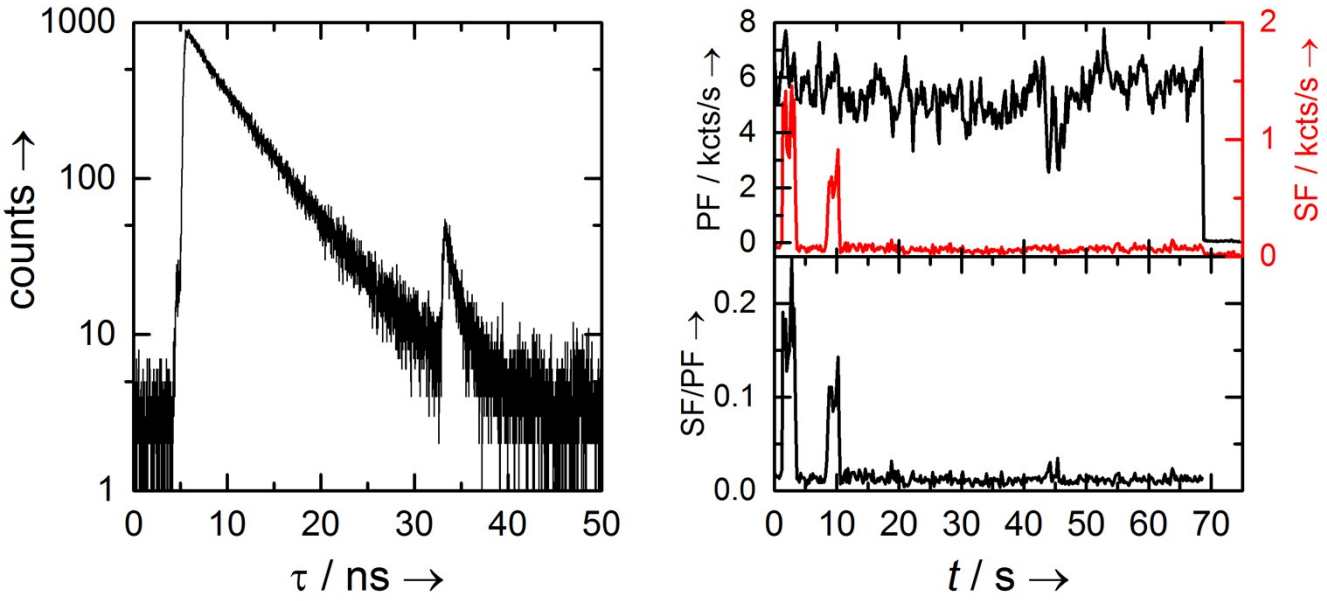

Figure S4: Example decay curve for a DNA-AgNC seemingly showing different τ_{PF} and τ_{SF}. The corresponding data point is shown in Figure 3A at $\tau_{PF} \approx 4.5$ ns and $\tau_{SF} \approx 1.5$ ns. The SF decay time is entirely dominated by two short bursts in the first 10 s. This time period is also accompanied by a high SF/PF ratio and a high SF intensity. Intriguingly, the PF intensity does not seem to change during the period of high SF signal, and we explain this observation by assuming that we have two independent DNA-AgNCs within the diffraction limited spot. One is constantly on, with a very low SF/PF ratio and constant PF signal, and the other one is mostly dark and only shows two bursts of high SF signal, with a very low PF signal and hence a very high SF/PF ratio.

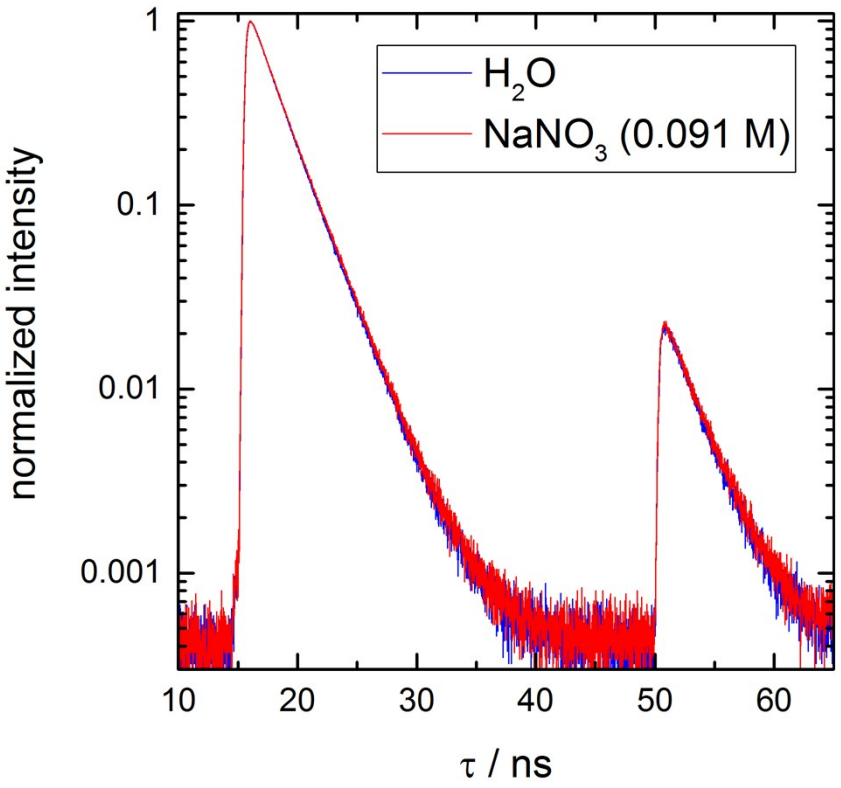

Figure S5: Fluorescence decay curves for DNA-AgNCs diluted in water (blue curve) and 0.091 M $NaNO_3$ (red curve) with the PF decay at 15 ns and the SF decay at 50 ns. Both samples were prepared by adding 5µl of the DNA-AgNCs dissolved in 10 mM NH_4OAc to 50µl of nuclease-free water (IDT) or 50µl of $NaNO_3$ (0.1M), respectively. As a result, the salt concentration should be different by about a factor of 100 between the two solutions. The primary excitation intensity was 5.8 kW/cm^2. The secondary excitation intensity was set to 785 kW/cm^2. The measurement time was 100 s.

Quantum yield clarification based on the scheme presented in Figure 1.

Quantum yield of dark state formation from primary excitation: Q_{D1}

$$Q_{D1} = k_{D1}/(k_{D1}+ k_{nr(FC)}+ k_{S1})$$

Quantum yield of emissive state formation from primary excitation: Q_{S1}

$$Q_{S1} = k_{S1}/(k_{D1}+ k_{nr(FC)}+ k_{S1})$$

Quantum yield of fluorescence from the S1 state: Q_F

$$Q_F = k_r/ (k_r+ k_{nr(S1)})$$

Quantum yield of fluorescence from primary excitation: Q

$$Q = Q_{S1}*Q_F = (k_{S1}/(k_{D1}+ k_{nr(FC)}+ k_{S1}))*(k_r/ (k_r+ k_{nr(S1)}))$$

Quantum yield of emissive state formation from the dark state: $Q_{D1\text{-}S1}$

$Q_{D1\text{-}S1}$ = not fully established at this point.

Quantum yield of OADF from primary and secondary excitation: Q_{OADF}

$Q_{OADF} = Q_{D1^*}Q_{D1\text{-}S1}$

References.

1. C. Cerretani, M. R. Carro-Temboury, S. Krause, S. A. Bogh and T. Vosch, *Chem. Commun.*, 2017, **53**, 12556-12559.
2. Z. Y. Liao, E. N. Hooley, L. Chen, S. Stappert, K. Mullen and T. Vosch, *J. Am. Chem. Soc.*, 2013, **135**, 19180-19185.